Nanocrystal Growth

DOI: 10.1002/anie.200705604

Quasi-Seeded Growth of Ligand-Tailored PbSe Nanocrystals through Cation-Exchange-Mediated Nucleation**

Maksym V. Kovalenko, Dmitri V. Talapin, Maria Antonietta Loi, Fabrizio Cordella, Günter Hesser, Maryna I. Bodnarchuk, and Wolfgang Heiss*

The solution-phase synthesis of inorganic nanocrystals (NCs) represents an efficient route towards a wide variety of compositions and morphologies at the nanoscale. A number of synthetic strategies are based on long-known or newly discovered phenomena in NC formation. The LaMer model, for example, introduced the idea of temporally separated nucleation and growth[1] and seeded growth.[2] Typically, balancing the nucleation and growth rates represents one of the major challenges in the colloidal synthesis of monodisperse NCs, as these processes have different activation energies and reaction orders. Balancing them in a one-pot reaction has proven to be sometimes very difficult (for example, in the case of GaAs).

The traditional approach is based on an empirical choice of the precursors, stabilizing agents, and reaction conditions. Alternatively, seeded growth allows nucleation and growth to be separated into two independently controlled steps. This approach works well for the synthesis of heterostructured (core–shell) NCs, in which the cores are used as nucleation centers for shell material that could be difficult to nucleate in a homogeneous solution (for example, Au/M (M = In, Sn, Bi),[3] or InAs/GaAs[4]). Unfortunately, the "seed" can alter the properties of the NCs, thus limiting the applications of seeded growth.

Herein, we report a novel approach for controlling the nucleation rate by generating intermediate nuclei, which quickly undergo an ion-exchange reaction that transforms them into the final product. This indirect nucleation pathway works only at the nanoscale, because of the possibility of very fast cation exchange in NCs.[5] We demonstrate that mediated nucleation followed by cation exchange can determine the overall nucleation rate and the final size of the NC. Furthermore, we show that synthesis in aliphatic amines allows the convenient surface derivatization of PbSe NCs with various ligands, which is not accessible by any of the previously reported synthetic approaches.

Colloidal NCs of narrow-bandgap semiconductors, such as PbSe, are of high interest because of their potential for applications[6] in electronic,[7] optical,[8] optoelectronic,[9] and thermoelectric devices.[10] The materials being explored at present include IV–VI (PbS, PbSe, PbTe, SnTe),[11] II–VI (HgTe),[12] and III–V (InAs)[4,13] compounds. As a result of the wide size-tunability of the bandgap energies, their absorption edges and photoluminescence (PL) bands cover the entire near-infrared (near-IR) spectral region up to mid-IR wavelengths of > 3 μm.[12b,14] In the case of Pb chalcogenides, other practically important properties are the large dielectric constants and Bohr radii[6,11d,e] and high carrier mobilities.[7]

In our preliminary experiments, we observed an efficient cation-exchange reaction during the treatment of preformed SnTe or SnSe NCs[11g] with $PbCl_2$ in oleylamine (OLA), as evidenced by the evolution of powder X-ray diffraction (XRD) patterns.[15] Herein, for the synthesis of monodisperse PbSe NCs, we perform cation exchange in situ during the nucleation stage by introducing $PbCl_2$ directly into the solution used for the synthesis of SnSe NCs.[11g] This leads to an interesting precursor-to-NC transformation pathway (Figure 1a). We chose OLA as coordinating solvent and trioctylphosphine selenide (TOPSe) as Se source.[1b] Note that the direct reaction between $PbCl_2$ and TOPSe typically yields very large and elongated PbSe particles[15] because of the very slow nucleation of PbSe, caused by insufficient reactivities of the precursors and by a high nucleation barrier. In contrast, addition of highly reactive bis[bis(trimethylsilyl)amino]-tin(II), $Sn[N(SiMe_3)_2]_2$, induces nearly instantaneous nucleation after the injection of the precursors.

In situ IR PL measurements were used to prove the immediate (≤ 1 s after injection) appearance of a bright PL signal, which indicates the formation of PbSe NCs (SnSe NCs are not luminescent because of their indirect energy gaps).[11g] Termination of the reaction a few minutes after the precursor injection yields monodisperse PbSe NCs (see Figure 1b and the Supporting Information) without application of any post-synthetic size selection. Importantly, the amount of PbSe NCs isolated from 50 mL of crude solution is as high as 1 g with a reaction yield of about 90% for small NC sizes (with respect to the initial amount of $PbCl_2$). The analysis of high-resolution transmission electron microscopy (HRTEM) images (see Figure 2b and the Supporting Information) and XRD patterns (Figure 2a) confirmed the cubic rock-salt crystal

[*] Dr. M. V. Kovalenko, G. Hesser, M. I. Bodnarchuk, Prof. W. Heiss
Institute of Semiconductor and Solid State Physics
University of Linz, Altenbergerstrasse 69, 4040 Linz (Austria)
Fax: (+43) 732-2468-9696
E-mail: maksym.kovalenko@jku.at
Prof. D. V. Talapin
Department of Chemistry
University of Chicago, Chicago, IL 60637 (USA)
Dr. M. A. Loi, Dr. F. Cordella
Physics of Organic Semiconductors
Zernike Institute for Advanced Materials
University of Groningen, 9747 AG Groningen (The Netherlands)

[**] Financial support from the Austrian Science Foundation FWF (START project Y179 and SFB-IRON) is gratefully acknowledged as well as technical support from the TSE department of the University Linz.

Supporting information for this article is available on the WWW under http://www.angewandte.org or from the author.

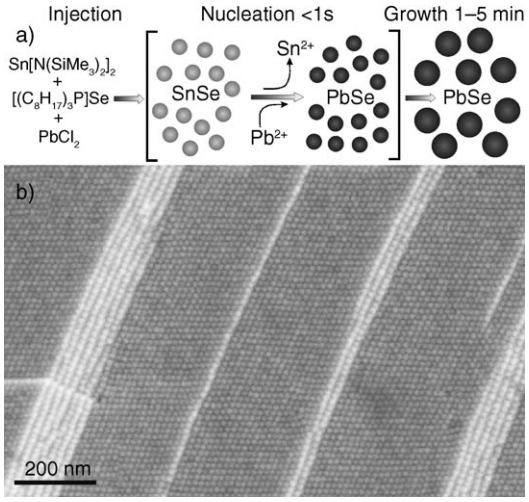

Figure 1. a) Cation-exchange-mediated nucleation of PbSe NCs followed by their growth. b) Scanning electron microscopy (SEM) image of a 3D NC superlattice of 13.8-nm PbSe NCs formed upon evaporation of a concentrated colloidal solution on an H-terminated Si substrate.

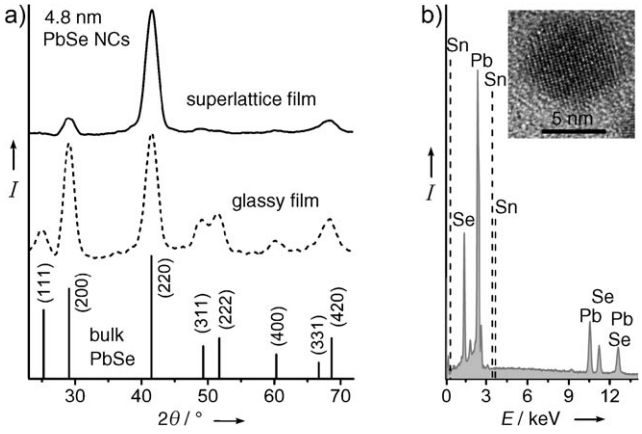

Figure 2. a) Powder XRD patterns of 4.8-nm PbSe NCs arranged into a superlattice (——) or glassy film (-----). b) EDX analysis of PbSe NCs; dashed lines are reference characteristic lines for Sn. Inset: typical HRTEM image of a 7.2-nm PbSe NC.

structure, identical to that of bulk PbSe (space group $Fm3m$, $a = 6.117$ Å). Energy-dispersive X-ray (EDX) analysis (Figure 2b) confirmed the stoichiometry of PbSe NCs without any detectable traces of Sn.

The mechanism for the nucleation of PbSe NCs described above (Figure 1a) can be verified by considering the dependence of the nucleation rate on the precursor concentration. In the framework of the classical nucleation theory, the nucleation rate is given by Eq. (1).[16]

$$\frac{dN}{dt} = A \exp\left(-\frac{\Delta G^N}{RT}\right) \quad (1)$$

Herein, $\Delta G^N = 16\pi\gamma^3 V_m^2/3(RT\ln S)^2$ is the activation free energy, A is the preexponential factor, γ is the specific surface energy, and V_m is the molar volume. S is the supersaturation, defined as the ratio between the monomer concentration $[M]_{bulk}$ and the monomer concentration in equilibrium with the bulk solid phase C^o_{bulk} (that is, solubility of the bulk solid) [Eq. (2)].

$$S = [M]_{bulk}/C^o_{bulk} \quad (2)$$

We can rewrite Equation (1) as [Eq. (3)], where $B = 16\pi\gamma^3 V_m^2/3(RT)^2$.

$$\ln\frac{dN}{dt} = \ln A - B/(\ln S)^2 \quad (3)$$

In the nucleation-controlled synthesis, that is, the synthesis where the Ostwald ripening is very slow and the final NC size is determined by the number of nuclei,[11b,g,16c] the final NC size is a good measure of the nucleation rate, $dN/dt \propto r^{-3}$ (r is the mean radius of the NC). S is determined by the concentration of the precursors participating in the nucleation step. We observed that the number of nuclei is determined exclusively by the concentration of $Sn[N(SiMe_3)_2]_2$ and TOPSe used for the nucleation reaction. If we vary only the concentration of $Sn[N(SiMe_3)_2]_2$ (denoted as [Sn]), $S \propto [Sn]$. Hence, Equation (3) predicts a linear dependence in coordinates $\ln(r^{-3})$ versus $(\ln[Sn])^{-2}$, which we indeed observed for the entire range of [Sn] used in the experiment (inset in Figure 3).

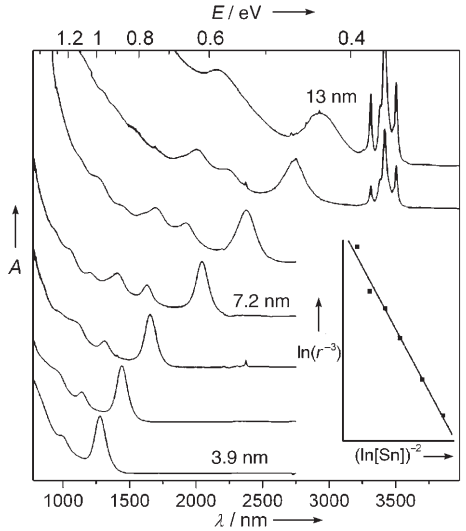

Figure 3. Room-temperature optical absorption spectra of PbSe NCs dispersed in tetrachloroethylene (TCE); 3.9–7.2-nm NCs were synthesized by varying the amount of $Sn[N(SiMe_3)_2]_2$ from 0.5 mL to 50 μL (for 0.7 mmol of $PbCl_2$ and 3 mmol of TOPSe). Larger NCs were obtained by additional injections of $PbCl_2$ and TOPSe into the solution containing 7.2-nm PbSe seeds. Sharp absorption lines around 3.3–3.5 μm represent C–H stretching vibrations of the surface ligands. Inset: experimentally obtained relationship between the amount of $Sn[N(SiMe_3)_2]_2$ and the size of the resulting PbSe NCs (linear plot for $\ln(r^{-3})$ versus $(\ln[Sn])^{-2}$).

An unusually fast cation-exchange reaction with molecule-like reaction kinetics is a remarkable feature of this new synthetic strategy. It cannot be explicitly explained by differ-

ences in the lattice free energies (3058 and 3050 kJ mol^{-1} for PbSe and SnSe, respectively).[17] We can distinguish two important factors that enable fast cation exchange in NCs. First is the size of the NCs, which matches the width of the reaction zone in solid-state reactions (4–5 nm).[5a] Second is the binding of the leaving Sn^{2+} cations by complexing agents (OLA in the present case). In terms of the Pearson theory of hard and soft acids and bases,[18] Sn^{2+} is a comparatively hard acid which readily binds with a hard base such as OLA, whereas Pb^{2+} is a softer acid. In accord with these arguments, no cation exchange occurs upon treatment of isolated SnSe or SnTe NCs with Pb^{2+}. A strong effect of complexing agents on the cation exchange in NCs has also been well documented by other groups.[5a–g,19]

The narrow size distribution of as-prepared PbSe NCs results in optical absorption spectra with multiple well-resolved electronic transitions (Figure 3). PbSe NCs with sizes ranging from 3.2 to 7.5 nm can be synthesized by tuning the concentration of $Sn[N(SiMe_3)_2]_2$ in the injection solution (lower four curves in Figure 3). Larger sizes (upper three curves in Figure 3) can be obtained by additional injections of $PbCl_2$/OLA and TOPSe into the crude solution of smaller PbSe NCs.

A similar tunability to that of the absorption edge is found in the PL spectra (Figure 4). The luminescence efficiencies of our samples generally follow the trend previously observed by

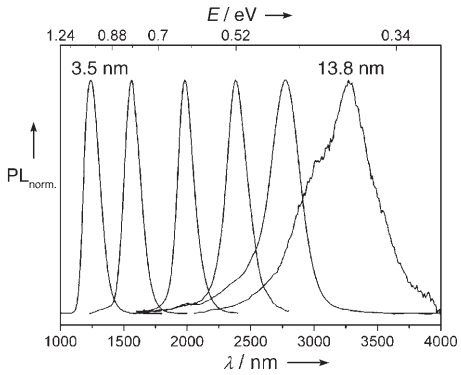

Figure 4. IR luminescence spectra (λ_{exc} = 980 nm) of PbSe NCs with sizes ranging from 3.5 to 13.8 nm dispersed in TCE.

Pietryga et al.[14] for PbSe NCs synthesized by the conventional oleate-based procedure: extremely high efficiencies of 30–80 % for the near-IR-emitting NCs drop to values of $\leq$ 1 % for mid-IR-emitting NCs. Narrow size distributions and high tendencies to 3D self-assembly are observed for the whole range of sizes (see Figure 1 b and the Supporting Information). Superlattices of PbSe NCs exhibit preferential crystallographic orientation of individual NCs, which is revealed by the enhancement of the (220) reflections in the XRD patterns (Figure 2 a). We did not notice a sphere-to-cube transition, which is commonly observed in Pb chalcogenide NCs.[11d,e]

The electronic states at the NC surface play an important role in carrier dynamics and they largely determine the optical and electronic characteristics of semiconductor NCs.[6–10] OLA appears to be a good leaving ligand for PbSe NCs, unlike oleic acid in the conventional oleate-based synthesis.[20] This enables the facile attachment of various ligands by adding a desired ligand directly to the NC solution. We attached various carboxylic acids (see Experimental Section), which provided high solubilities of NCs in nonpolar solvents if the chain length was at least nine carbon atoms.

As an even shorter ligand we used pyridine, known as an efficient intermediate ligand that dynamically binds to the surface of CdSe NCs.[1b] Importantly, different surface cappings result in very similar absorption and emission spectra of colloidal solutions of PbSe NCs.[15] Pyridine does not quench the band-edge luminescence of PbSe NCs. Time-resolved PL measurements on colloidal solutions of 3.1-nm PbSe NCs show lifetimes ($\tau_{1/e}$) of 1.5 and 0.16 μs for oleate- and pyridine-capped NCs, respectively (see Figure 5 a and the Supporting Information).

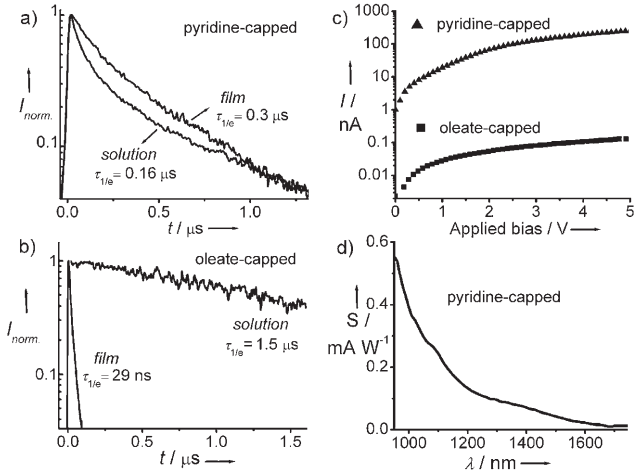

Figure 5. a) Luminescence decays for 3.1-nm PbSe NCs in solutions and in films capped by a) pyridine and b) oleic acid. c) Current–voltage (*I*–*V*) characteristics of the films formed by 5.1-nm oleate- and pyridine-capped PbSe NCs. d) Sensitivity spectrum at a bias voltage of 5 V from the device consisting of an approximately 0.5 μm-thick film of 5.1-nm pyridine-capped NCs deposited on an interdigitated structure of gold electrodes (20 μm channel length) on glass.

In general, the long lifetimes in Pb chalcogenide NCs are attributed to the effect of internal dielectric screening on the radiative recombination rate.[11d,21] In films, the oleate-capped NCs exhibit much shorter radiative lifetimes ($\tau_{1/e}$ = 29 ns, see the Supporting Information) similar to those previously reported for PbS[11c] and PbSe NCs.[22] This observation can be attributed to an increase of nonradiative recombination as a result of interparticle charge- and energy-transfer processes[23] and/or through the surface traps formed upon film preparation.[24] Strikingly higher lifetimes ($\tau_{1/e}$ = 0.3 μs) are observed, however, in the PL decays from the films of pyridine-capped NCs (Figure 5 c). Moreover, the PL quantum efficiencies are also much higher in the films of pyridine-capped dots as compared to the films of PbSe NCs capped with carboxylic acids.[15]

As a result of the much smaller length of the pyridine molecule (ca. 0.3 nm) compared to C_9–C_{18} carboxylic acids (ca. 1.1–2.1 nm), films of pyridine-capped PbSe NCs exhibit higher electrical conductivities by a factor of 10^3–10^4 (Figure 5b). Furthermore, the improved charge transport, longer carrier lifetimes in films, and the tunable absorption spectra in the near-IR region make pyridine-capped PbSe NCs very promising for applications in optoelectronic devices, such as IR photodetectors. Figure 5d shows the sensitivity spectrum from the photoconductor made of 5.1-nm pyridine-capped PbSe NCs deposited on an interdigitated electrode structure. With a current noise of 0.2 $pA\,Hz^{-1/2}$, such devices exhibit a detectivity of $D^* = 5 \times 10^8\,cm\,Hz^{1/2}\,W^{-1}$ at a wavelength of 1 μm and illumination power of 2.5 $\mu W\,cm^{-2}$, measured at a modulation frequency of 33 Hz.

Furthermore, we examined the applicability of the Sn^{2+}-to-Pb^{2+} cation exchange to the nucleation of monodisperse PbTe NCs. By only replacing TOPSe with TOPTe, we produced very small (ca. 1.9 nm) and highly luminescent (PL maximum at 950 nm) PbTe NCs.[15] Such a strong decrease in size compared to PbSe NCs synthesized under very similar conditions can be explained by the higher reactivity of TOPTe. These NCs are also significantly smaller than the NCs produced by the conventional oleate-based approach.[11e,f]

In summary, we have developed a new concept for controlling the nucleation of monodisperse colloidal NCs. We have demonstrated that the high reactivity of the precursor for one metal (Sn) can be converted into an efficient nucleation of NCs containing another metal (PbSe) through the cation-exchange reaction. The results support the hypothesis that cation exchange can be extremely fast and complete in small NCs. As a model system, we synthesized monodisperse PbSe NCs, and also very small PbTe NCs. The synthesis also enabled better control over the surface chemistry of PbSe NCs, which is of practical importance for various electronic and optoelectronic applications. Mediated nucleation followed by cation exchange can be a very useful synthetic strategy in systems with a high barrier for homogeneous nucleation, such as GaAs, $BaTiO_3$, and some other NCs.

Experimental Section

Standard airless techniques (Schlenk line and nitrogen glove box) were used in the synthesis of PbSe NCs. $PbCl_2$ (0.19 g, 99.999%, Aldrich) was dissolved in OLA (7 mL, technical grade, Aldrich) and the mixture was heated under vacuum at 100 °C for 15 min. In a glove box, $Sn[N(SiMe_3)_2]_2$ (50–750 μL for 5.5–3.2-nm PbSe NCs; Aldrich) was dissolved in trioctylphosphine (TOP; 1 mL, 97%, Strem), mixed with a 10% solution of Se in TOP (3 mL), and loaded into a syringe. Subsequently, the contents of the syringe were injected into a $PbCl_2$/OLA solution at 140 °C, and the reaction flask was kept at 120 °C for 2 min and then rapidly cooled to room temperature. For the synthesis of 5.5–7.5-nm PbSe NCs, the injection and growth temperatures were raised to 160 and 140 °C, respectively, to increase the sizes of the initial nuclei. For the synthesis of 7.5–14-nm PbSe NCs, additional multiple injections of $PbCl_2$/OLA (prepared in a separate flask) and TOPSe were performed in small portions at 140 °C over 0.5 to 2 h.

Surface functionalization and isolation of PbSe NCs: For the preparation of pyridine-capped NCs, OLA-capped PbSe NCs were precipitated from the crude solution by addition of ethanol. The precipitate was separated by centrifugation and the NCs were redissolved in pyridine to form stable colloidal solutions. The NCs were additionally purified with hexane/pyridine as nonsolvent and solvent, respectively. Attachment of C_9–C_{18} carboxylic acids was performed by direct addition of the corresponding acid to the crude solution (ca. 20% by weight) of OLA-capped PbSe NCs, followed by stirring for 15 min. The NCs were isolated with chloroform/ethanol as a solvent/nonsolvent pair.

TEM and HRTEM images were obtained with a JEOL 2011 microscope operating at an acceleration voltage of 200 kV. EDX elemental analysis was performed on a JEOL JSM-6400 scanning electron microscope. SEM images were acquired using a Zeiss 1540XB microscope. Wide-angle powder XRD patterns were collected using a Bruker D8 diffractometer with a GADDS area detector. The *I–V* characteristics were acquired with a Keithley 236 source–measure unit. The photocurrent spectra were recorded by a lock-in technique using a Stanford Research SR510 lock-in amplifier, a Xe lamp, and a 0.15-m SpectraPro monochromator (Acton). Noise currents were measured using the same lock-in amplifier. Sensitivities were estimated after the measurement of the source power spectrum using a pyrometer. Linear optical absorption spectra were obtained with a BOMEM DA8 Fourier-transform infrared spectrometer operating from 10000 to 400 cm^{-1}. PL was excited by an InGaAs laser diode at 980 nm, dispersed with a 0.15-m SpectraPro monochromator, and acquired by an InSb detector. For time-resolved PL measurements, the samples were excited at 800 nm by 100-fs pulses delivered by a mode-locked Ti:sapphire laser (Coherent, Mira 900), and an optical pulse selector (APE, Pulse Select) was used to vary the repetition frequency of the exciting pulse train between 4 MHz and 50 kHz. A streak camera (Hamamatsu M5677) working in single-sweep mode coupled with an imaging spectrometer was employed to collect time-resolved PL spectra.

Received: December 7, 2007
Published online: March 12, 2008

Keywords: crystal growth · ion exchange · luminescence · nanostructures · semiconductors

[1] a) V. K. LaMer, R. H. Dinegar, *J. Am. Chem. Soc.* **1950**, *72*, 4847–4854; b) C. B. Murray, D. J. Norris, M. G. Bawendi, *J. Am. Chem. Soc.* **1993**, *115*, 8706–8715; c) Z. A. Peng, X. Peng, *J. Am. Chem. Soc.* **2002**, *124*, 3343–3353.

[2] a) N. R. Jana, L. Gerheart, C. J. Murphy, *Chem. Mater.* **2001**, *13*, 2313–2322; b) J. Park, E. Lee, N. M. Hwang, M. Kang, S. C. Kim, Y. Hwang, J. G. Park, H. J. Noh, J. Y. Kim, J. H. Park, T. Hyeon, *Angew. Chem.* **2005**, *117*, 2932–2937; *Angew. Chem. Int. Ed.* **2005**, *44*, 2872–2877; c) S. E. Habas, H. Lee, V. Radmilovic, G. A. Somorjai, P. Yang, *Nat. Mater.* **2007**, *6*, 692–697; d) S. H. Im, Y. T. Lee, B. Wiley, Y. Xia, *Angew. Chem.* **2005**, *117*, 2192–2195; *Angew. Chem. Int. Ed.* **2005**, *44*, 2154–2157; e) H. Yu, M. Chen, P. M. Rice, S. X. Wang, R. L. White, S. Sun, *Nano Lett.* **2005**, *5*, 379–382.

[3] H. Yu, P. C. Gibbons, K. F. Kelton, W. E. Buhro, *J. Am. Chem. Soc.* **2001**, *123*, 9198–9199.

[4] J. W. Cao, U. Banin, *J. Am. Chem. Soc.* **2000**, *122*, 9692–9702.

[5] a) D. H. Son, S. M. Hughes, Y. Yin, A. P. Alivisatos, *Science* **2004**, *306*, 1009–1012; b) U. Jwong, J.-U. Kim, Y. Xia, Z.-Y. Li, *Nano Lett.* **2005**, *5*, 937–942; c) L. Dloczik, R. Könenkamp, *Nano Lett.* **2003**, *3*, 651–653; d) R. D. Robinson, B. Sadtler, D. O. Demchenko, C. K. Erdonmez, L.-W. Wang, A. P. Alivisatos, *Science* **2007**, *317*, 355–358; e) M. T. Harrison, S. V. Kershaw, M. G. Burt, A. Eychmüller, H. Weller, A. L. Rogach, *Mater. Sci. Eng. B* **2000**, *69–70*, 355–360; f) C. R. Lubeck, T. Y.-J. Han, A. E. Gash, J. H. Satcher, Jr., F. M. Doyle, *Adv. Mater.* **2006**, *18*, 781–784;

g) W. Zhu, W. Wang, J. Shi, *J. Phys. Chem. B* **2006**, *110*, 9785 – 9790.
[6] A. L. Rogach, A. Eychmüller, S. G. Hickey, S. V. Kershaw, *Small* **2007**, *3*, 536 – 557, and references therein.
[7] D. V. Talapin, C. B. Murray, *Science* **2005**, *310*, 86 – 89.
[8] a) R. D. Schaller, M. A. Petruska, V. I. Klimov, *J. Phys. Chem. B* **2003**, *107*, 13765 – 13768; b) E. Lifshitz, M. Brumer, A. Kigel, A. Sashchiuk, M. Bashouti, M. Sirota, E. Galun, Z. Burshtein, A. Q. Le Quang, I. Ledoux-Rak, J. Zyss, *J. Phys. Chem. B* **2006**, *110*, 25356 – 25365.
[9] a) G. Konstantatos, I. Howard, A. Fischer, S. Hoogland, J. Clifford, E. Klem, L. Levina, E. H. Sargent, *Nature* **2006**, *442*, 180 – 183; b) S. A. Mcdonald, G. Konstantanos, S. Zhang, P. W. Cyr, E. J. D. Klem, L. Levina, E. H. Sargent, *Nat. Mater.* **2005**, *4*, 138 – 142; c) M. Böberl, M. V. Kovalenko, S. Gamerith, E. List, W. Heiss, *Adv. Mater.* **2007**, *19*, 3574 – 3578; d) J. S. Steckel, S. Coe-Sullivan, V. Bulovic, M. G. Bawendi, *Adv. Mater.* **2003**, *15*, 1862 – 1866.
[10] M. S. Dresselhaus, G. Chen, M. Y. Tang, R. Yang, H. Lee, D. Wang, Z. Ren, J.-P. Fleurial, P. Gogna, *Adv. Mater.* **2007**, *19*, 1043 – 1053.
[11] a) C. B. Murray, S. Sun, W. Gaschler, H. Doyle, T. A. Betley, C. R. Kagan, *IBM J. Res. Dev.* **2001**, *45*, 47 – 55; b) M. A. Hines, G. D. Scholes, *Adv. Mater.* **2003**, *15*, 1844 – 1849; c) L. Cademartiri, J. Bertolotti, R. Sapienza, D. S. Wiersma, G. Freymann, G. A. Ozin, *J. Phys. Chem. B* **2006**, *110*, 671 – 673; d) B. L. Wehrenberg, C. Wang, P. Guyot-Sionnest, *J. Phys. Chem. B* **2002**, *106*, 10634 – 10640; e) J. E. Murphy, M. C. Beard, A. G. Norman, S. P. Ahrenkiel, J. C. Johnson, P. Yu, O. Micic, R. J. Ellingson, A. Nozik, *J. Am. Chem. Soc.* **2006**, *128*, 3241 – 3247; f) J. J. Urban, D. V. Talapin, E. V. Shevchenko, C. B. Murray, *J. Am. Chem. Soc.* **2006**, *128*, 3248 – 3255; g) M. V. Kovalenko, W. Heiss, E. V. Shevchenko, J.-S. Lee, H. Schwinghammer, A. P. Alivisatos, D. V. Talapin, *J. Am. Chem. Soc.* **2007**, *129*, 11354 – 11355.
[12] a) A. Rogach, S. Kershaw, M. Burt, M. Harrison, A. Kornowski, A. Eychmüller, H. Weller, *Adv. Mater.* **1999**, *11*, 552 – 555; b) M. V. Kovalenko, E. Kaufmann, D. Pachinger, J. Roither, M. Huber, J. Stangl, G. Hesser, F. Schaffler, W. Heiss, *J. Am. Chem. Soc.* **2006**, *128*, 3516 – 3517.
[13] S.-W. Kim, J. P. Zimmer, S. Ohnishi, J. B. Tracy, J. V. Frangioni, M. B. Bawendi, *J. Am. Chem. Soc.* **2005**, *127*, 10526 – 10532.
[14] J. M. Pietryga, R. D. Schaller, D. Werder, M. H. Stewart, V. I. Klimov, J. A. Hollingsworth, *J. Am. Chem. Soc.* **2004**, *126*, 11752 – 11753.
[15] For additional details, see the Supporting Information.
[16] a) J. W. Mullin, *Crystallization*, 3rd ed., Oxford University Press, Oxford, **1997**; b) J. Park, J. Joo, S. G. Kwon, Y. Jang, T. Hyeon, *Angew. Chem.* **2007**, *119*, 4714 – 4745; *Angew. Chem. Int. Ed.* **2007**, *46*, 4630 – 4660; c) E. V. Shevchenko, D. V. Talapin, H. Schnablegger, A. Kornowski, O. Festin, P. Svedlindch, M. Haase, H. Weller, *J. Am. Chem. Soc.* **2003**, *125*, 9090 – 9101.
[17] *CRC Handbook of Chemistry and Physics*, 70th ed., CRC Press, Boca Raton, **1990**.
[18] R. G. Pearson, *J. Am. Chem. Soc.* **1963**, *85*, 3533 – 3539.
[19] P. H. C. Camargo, Y. H. Lee, U. Jeong, Z. Zou, Y. Xia, *Langmuir* **2007**, *23*, 2985 – 2992.
[20] As a result of the weak ligand binding, OLA-capped PbSe NCs show very low solubility after the first precipitation from the crude solution, whereas surface capping by oleic acid significantly improves the colloidal stability.
[21] J. M. An, A. Franceschetti, A. Zunger, *Nano Lett.* **2007**, *7*, 2129 – 2135.
[22] M.-H. Lee, W. J. Chung, S. K. Park, M.-S. Kim, H. S. Seo, J. J. Ju, *Nanotechnology* **2005**, *16*, 1148 – 1152.
[23] C. R. Kagan, C. B. Murray, M. G. Bawendi, *Phys. Rev. Lett.* **1996**, *54*, 8633 – 8643.
[24] J. M. Luther, M. C. Beard, Q. Song, M. Law, R. J. Ellingson, A. J. Nozik, *Nano Lett.* **2007**, *7*, 1779 – 1784.

